Mutagenesis of Two Acidic Active Site Residues in Human Muscle Creatine Kinase: Implications for the Catalytic Mechanism†

John S. Cantwell,‡ Walter R. Novak,‡ Pan-Fen Wang,§ Michael J. McLeish,§ George L. Kenyon,§ and Patricia C. Babbitt*,‡

Departments of Biopharmaceutical Sciences and Pharmaceutical Chemistry, School of Pharmacy, University of California, San Francisco, California 94143-0446, College of Pharmacy, University of Michigan, Ann Arbor, Michigan 48109-1065

Received September 6, 2000; Revised Manuscript Received January 17, 2001

ABSTRACT: Creatine kinase (CK) catalyzes the reversible phosphorylation of the guanidine substrate, creatine, by MgATP. Although several X-ray crystal structures of various isoforms of creatine kinase have been published, the detailed catalytic mechanism remains unresolved. A crystal structure of the CK homologue, arginine kinase (AK), complexed with the transition-state analogue (arginine-nitrate-ADP), has revealed two carboxylate amino acid residues (Glu225 and Glu314) within 2.8 Å of the proposed transphosphorylation site. These two residues are the putative catalytic groups that may promote nucleophilic attack by the guanidine amino group on the γ-phosphate of ATP. From primary sequence alignments of arginine kinases and creatine kinases, we have identified two homologous creatine kinase acidic amino acid residues (Glu232 and Asp326), and these were targeted for examination of their potential roles in the CK mechanism. Using site-directed mutagenesis, we have made several substitutions at these two positions. The results indicate that of these two residues the Glu232 is the likely catalytic residue while Asp326 likely performs a role in properly aligning substrates for catalysis.

Creatine kinase (CK;[1] EC 2.7.3.2) is responsible for the production and maintenance of a "high-energy" phosphate intermediate, phosphocreatine (PCr), that can be converted to ATP in cells requiring short, rapid bursts of energy. The isoforms of CK are named for the tissues and organelles with high-energy demands in which they were originally and predominantly found, namely the muscle [M-type (*1*)], brain [B-type (*2*)], and mitochondrial [Mt-type (*3*)] CK isozymes. Because of its central importance in cellular metabolism, cellular CK concentrations and/or activity are perturbed in a wide range of human disease states, including cardiac infarct (*4*), cancer (*5*−*7*), muscular dystrophies (*8*), and neurodegenerative diseases (*9*, *10*).

CK has been a topic of active research efforts for over 50 years and serious investigations of its mechanism have spanned at least the last 30. The advances in understanding of the mechanism have coincided with the advent of new techniques. Cross-linking and affinity labeling studies have implicated a reactive cysteine [Cys283, HMCK numbering (*11*, *12*)], as well as lysine (*13*, *14*) and arginine residues (*15*) that interact with negatively charged phosphates of the substrates. In addition to cross-linking studies (*16*, *17*), NMR investigations (*18*) have suggested a reactive histidine, while pH profile data have suggested the presence of a catalytic histidine residue together with an assisting carboxylate (*19*).

Nearly two decades later, site-directed mutagenesis has been employed to confirm, modify, or reject the suspected mechanistic importance of some of these residues. For example, mutagenesis studies of the so-called "essential" cysteine (Cys283) show that significant activity can be retained even after amino acid substitution (*20*, *21*). In other cases, little or no activity is observed when this residue is replaced (*11*). However, despite these many investigations, the precise catalytic role of the cysteine remains to be determined. More readily interpreted results confirm that both arginine (*21*) and tryptophan (*22*−*24*) residues function as nucleotide-binding groups. Finally, mutagenesis of all five highly conserved histidine residues have excluded a centrally important catalytic function for any of them (*25*). This result strongly suggests that the long-held model of the chemical mechanism, which involves a histidine residue acting as a potential general base, must now be reevaluated.

The recent solution of several crystal structures of CK, including ubiquitous mitochondrial CK from chicken heart [uMtCK (*26*)], rabbit muscle CK [RMCK (*27*)], chicken brain b-form CK (*28*), and human ubiquitous mitochondrial CK (*3*), provides evidence confirming the roles of many residues previously implicated in substrate-binding or dimer and tetramer formation and/or stabilization. Unfortunately, however, no crystal structure of CK bound to either substrate or product analogues is yet available. Thus, the primary players in the CK mechanism, the catalytic residues (and therefore the details of the CK mechanism) remain largely

* To whom correspondence should be addressed.
† Supported by USPHS Grant AR17323 to GLK and PCB.
‡ University of California.
§ University of Michigan.

[1] Abbreviations: CK, creatine kinase; HMCK, human muscle creatine kinase; AK, arginine kinase; TSAC, transition-state analogue complex; RMCK, rabbit muscle creatine kinase; MtCK, mitochondrial creatine kinase; sMtCK, sarcomeric mitochondrial creatine kinase; uMtCK, ubiquitous mitochondrial creatine kinase; LB medium, Luria-Bertani medium; CyCr, cyclocreatine; ORF, open reading frame; EDTA, ethylenediaminetetraacetic acid; PMSF, phenylmethanesulfonyl fluoride; SDS−PAGE, sodium dodecyl sulfate polyacrylamide gel electrophoresis.

10.1021/bi0020980 CCC: $20.00
Published on Web 02/16/2001

unidentified. To some extent, this problem has been ameliorated by the recent publication of an arginine kinase structure (AK-TSAC) complexed with a transition-state analogue, arginine-nitrate-ADP (*29*). Arginine kinase (AK; EC 2.7.3.3) and CK are structurally similar members of the guanidino-kinase family, exhibit ~40% identity in their amino acid sequences, and show high levels of sequence conservation for all residues/motifs known to be functionally important. The structure of this liganded AK is superimposable upon the unliganded structure of RMCK at an RMSD of 1.25 Å over 236 of 381 total α-carbons. Given these similarities, the AK-TSAC structure can be used as an approximate model of the CK active site. As described by Zhou et al. (*29*), two arginine kinase carboxylate residues, Glu 225 and Glu 314, are located in an ideal position to facilitate proton donation and/or abstraction from the $N_{\eta 1}$ and $N_{\eta 2}$ amine groups of arginine. In human muscle CK, the analogous carboxylates are Glu232 and Asp326, respectively. To provide insight concerning how the cytosolic CKs function at the molecular level, we have chosen to examine the human muscle variant of CK, both because it is important to human health and because it is highly similar (96% identity) to the enzyme from rabbit muscle (RMCK), the form on which most of the previous mechanistic work has been done. In this paper, we describe the replacement of each of these carboxylates with residues that are either functionally or structurally homologous. The results of these substitutions are compared with those from a nonconservative substitution, also generated for each of these carboxylates. Using this system, we can evaluate the roles of the carboxylates in both substrate binding and catalysis.

MATERIALS AND METHODS

Materials. Unless otherwise stated, chemicals and reagents were purchased from either Fisher Scientific or Aldrich-Sigma Chemicals. Restriction enzymes were purchased from New England Biolabs.

Bacterial Strains and Vectors. HMCK wild-type construct was created as previously described (*30*). HMCK mutant plasmid DNA was transformed into DH5α cells (Gibco BRL) for mutant construction, propagation, and sequencing.

Site-Directed Mutagenesis. Amino acid substitutions were created using the QuikChange kit (Stratagene), with mutagenic primers containing unique restriction site identifiers. Plasmids were purified using the NucleoSpin Plus Miniprep kit (Clontech), and mutant clones were identified by restriction site analysis. Sequence confirmation and oligonucleotide primer synthesis were performed by the Biomolecular Resource Center (BRC, University of California, San Francisco).

Growth and Overexpression. Plasmids containing the HMCK gene were transformed into BL21(DE3)pLysS cells (Stratagene) and spread onto LB agar plates containing carbenicillin (50 μg/mL) and chloramphenicol (34 μg/mL). Single colonies were used to inoculate 1−2 L of LB medium containing the appropriate antibiotics. Cells were grown in an incubator/shaker at 37 °C to an absorbance reading (A_{600}) of 0.8−1.0 at which point IPTG (0.4 mM) was added and the flasks were cooled to 20 °C for overnight growth (~15 h). Cells were harvested by centrifugation (15 min at 5000*g*), the cell pellet (~2.5−5 g/L) was washed with 25 mM Tris buffer, pH 7.5, collected and stored at −20 °C.

Purification. Cells were lysed in 25 mM Tris, 50 mM NaCl, 5 mM EDTA, and 0.1 mM PMSF by lysozyme treatment (0.3 mg/mL), three freeze−thaw cycles, and sonication. The cell lysate was centrifuged (30 min at 100000*g*), and the supernatant passed over a Q-Sepharose (Amersham-Pharmacia) anion-exchange column equilibrated with 25 mM Tris buffer, pH 7.0. CK eluted with the flow-through fraction. This fraction was then applied to a Blue Sepharose (Amersham-Pharmacia) dye affinity column which had been equilibrated in 20 mM MOPS buffer, pH 7.0. A 50 to 500 mM NaCl gradient was applied, and CK eluted between 200 and 300 mM NaCl. Fractions containing CK were combined and concentrated using an Amicon concentrator fitted with 30K molecular weight cutoff membrane.

Protein Concentration and Determination of Purity. Protein concentration was determined by the Bradford assay (*31*) with bovine serum albumin as the protein standard. Purity was determined by SDS−PAGE. NuPAGE 10% Bis-Tris precast gels (Invitrogen-Novex) were used with MOPS, pH 7.0, running buffer per manufacturer's instructions. CK-bands at 43 kDa represented ≥95% of the total protein per lane as determined by densitometry. Native gels were used to verify dimerization and charge shift of mutant CKs. NuPAGE 7% Tris-acetate precast gels were run with Tris-glycine native running and sample buffer per manufacturer's instructions.

Enzyme Assays. Creatine kinase activity was determined at 30 °C in the forward direction (PCr formation) by the NADH-linked assay method (*32*). The reverse direction (ATP production) was measured by the NADP-linked assay method (*33*). V_{max} and K_m values were calculated using Hyper.exe, a hyperbolic regression analysis program (version 1.0, copyright J. S. Easterby, 1992). Cyclocreatine, synthesized as previously described (*34*), was a kind gift of Dr Liangren Zhang.

Structural Superpositions. Structural superpositions were generated using MinRMS (*35*). The superpositions of creatine kinase (1CRK, A chain only) and arginine kinase (1BGO) were visualized using Chimera and the Chimera extension, AlignPlot (*35*). The superposition aligns 236 α-carbons with an average RMSD of 1.25 Å. The graphic shown in Figure 2 was created using MidasPlus (*36*).

RESULTS

Sequence Homology. Figure 1 presents the primary sequence alignments of several species and isoforms of CK and AK in the regions of interest. The first region, residues 223−243 (numbered using the HMCK sequence), shows high sequence similarity among all known guanidino kinases, and includes a region we have designated the "NEED-box". This region is highlighted in Figure 1. A second region, HMCK residues 316−338 in Figure 1, has been identified in several of the guanidino kinase superfamily structure studies as containing an active-site flexible loop. This flexible loop, also highlighted in Figures 1 and 2 (HMCK residues 323−330), has been associated with a conformational change that occurs upon substrate binding (*37*). Two putative bacterial guanidino-kinase ORFs (*Bacillus subtilis* and *Listeria monocytogenes*) have been included in the alignments in order to

	223	243	316	338
MCK human	KSFLVWVNEEDHLRVISMEKG		RLQKRGTGGVDTAAVGSVFDVSN	
MCK rabbit	KSFLVWVNEEDHLRVISMEKG		RLQKRGTGGVDTAAVGSVFDISN	
MCK mouse	KSFLVWVNEEDHLRVISMEKG		RLQKRGTGGVDTAAVGAVFDISN	
T. californica CK	KTFLVWVNEEDHLRVISMQKG		RLQKRGTGGVDTAAVGSIYDISN	
BCK human	KTFLVWVNEEDHLRVISMQKG		RLQKRGTGGVDTAAVGGVFDVSN	
BCK mouse	KTFLVWINEEDHLRVISMQKG		RLQKRGTGGVDTAAVGGVFDVSN	
sMtCK human	KSFLIWVNEEDHTRVISMEKG		RLQKRGTGGVDTAATGGVFDISN	
uMtCK chicken	KTFLIWINEEDHTRVISMEKG		RLQKRGTGGVDTAATANVFDISN	
uMtCK human	KTFLIWINEEDHTRVISMEKG		RLQKRGTGGVDTAAVADVYDISN	
AK horseshoe crab	KTFLVWVNEEDHLRIISMQKG		NLQVRGTRGEHTESEGGVYDISN	
AK grasshopper	KTFLVWCNEEDHLRIISMQMG		SLQVRGTRGEHTEAEGGIYDISN	
AK honeybee	KTFLVWCNEEDHLRIISMQMG		NLQVRGTRGEHTEAEGGIYDISN	
AK Drosophila	KTFLVWCNEEDHLRIISMQQG		YNLQVANPREHTEAEGGSYDISN	
AK lobster	KTFLVWCNEEDHLRIISMQPG		NLQVRGSTGEHTEAEGGVYDISN	
Lombricine Kinase	KTFLIWINEEDQVRIIAMQHG		HLQKRGTGGEHTEAVDDVYDISN	
Glycocyamine Kinase	KNFLVWINEEDHIRIISMQKG		RLGKRGTGGESSLAEDSTYDISN	
B. subtilis	EEVSVMLNEEDHIRIQCLFPG		GLVVRGIYGEGSEAVGNIFQISN	
L. monocytogenes	ENVSIMLNEEDHLRIQCMTPG		GFVVRGIYGEGSMPASNIFQVSN	

FIGURE 1: Multiple sequence alignment of important regions of several guanidino-kinases proposed to contain active-site residues. Alignments were generated using ClustalW (*46*). Regions of interest as described in the text are highlighted in yellow, and conserved carboxyl residues, based on structural alignments, are marked with arrows. Residue numbering is based on the HMCK sequence. For the flexible loop region, residues specific to CK specific are in blue and residues specific to AK are in magenta. MCK human, gi125305; MCK rabbit, gi125307; MCK mouse, gi125306; T. californica CK, gi125309; BCK human, gi125294; BCK mouse, gi417208; sMtCK human, gi125312; uMtCK chicken, gi2497494; uMtCK human, gi125315; AK horseshoe crab, gi1708613; AK grasshopper, gi1688218; AK honeybee, gi7434587; AK Drosophila, gi1346366; AK lobster, gi585342; Lombricine Kinase, gi3183058; Glycocyamine Kinase, gi1730042; B. subtilis, gi2127054; L. monocytogenes, gi1314296.

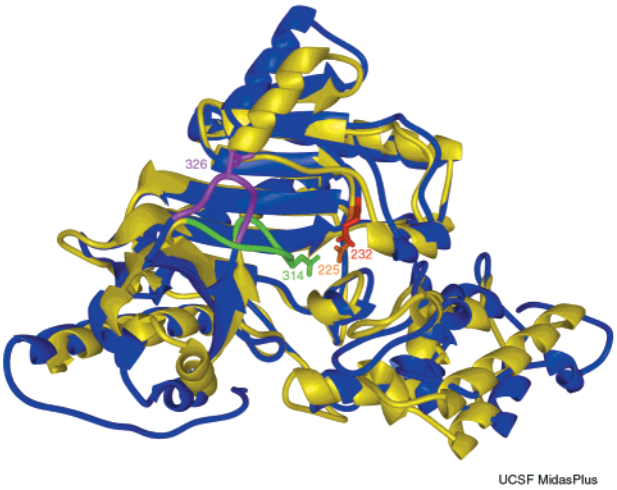

FIGURE 2: Structural superposition of uMtCK and AK. uMtCK α-carbon trace is in blue, while AK is in yellow. The CK flexible loop is in purple, the AK loop is in green. Glu225 of the AK structure is colored orange while the CK Glu 232 is in red.

contrast the relative homology between and within species and isozymes for AKs and CKs. The NEED-box represents a highly conserved motif across all of these sequences with ~80% identity for each pairwise comparison in this region. The highlighted NEED-box region has only one amino acid difference among all of the sequences shown, including the very distantly related bacterial ORFs. By contrast, the flexible loop exhibits much more variability across the alignment, with all CKs highly similar to each other, all AKs highly similar to each other, but with only 38% identity between CKs and AKs. Within a core of eight residues that surround the AK Glu314 or CK Asp326 position there is a distinct variation of side-chain properties for four of the eight residues. In CK there is a predominance of small nonpolar groups (Gly323, Val325, Ala328, and Val330), whereas the corresponding AK residues are charged (Arg312, His315, Glu317, and Glu319).

Purification. Wild-type and mutant HMCKs display nearly identical elution profiles from Blue-Sepharose. SDS−PAGE analysis reveals similar levels of yield, purity and subunit migration distances (data not shown). In a native gel, the E232D and D326E mutants comigrate with wild-type HMCK, while the E232Q and E232A also comigrate with each other, but at a slower rate than wild-type HMCK. Finally, the D326N and D326A variants have identical (to each other) but even slower migration behavior. Conspicuous differences in these native gel migration patterns of the purified mutant and wild-type HMCKs presumably are attributable to charge differences.

Kinetics. Functionally-, structurally-, and nonconservative amino acid substitutions, generated at each of the two residues, E232 and D326, led to large differences in their respective V_{max} values (Table 1). A functionally conservative substitution at the Glu232 position (E232D) results in a 500-fold loss of activity, while the comparable mutation at Asp326 (D326E) results in only a 3-fold loss in activity. Structurally conservative substitution results in a nearly 100000-fold decrease in activity for E232Q, while the D326N construct produces only a 20-fold decrease in catalytic rate. Last, the nonconservative E232A substitution completely eliminates detectable enzymatic activity, while the analogous variant, D326A, retains 0.1% of wild-type activity. In agreement with previously published values (*38*), the reverse reaction activity rates are 2−3 times higher than the forward

Table 1: Maximum Specific Activity[a] and Michaelis Constants[b] for Wild-Type and Recombinant HMCKs

protein	V_{max} forward (units/mg)	V_{max} reverse (units/mg)	K_m^{Cr}	K_m^{ATP}	K_m^{PCr}	K_m^{ADP}
wild-type	114 ± 7.4	304 ± 6.0	10.3 ± 2.4	0.504 ± 0.11	0.714 ± 0.061	0.0484 ± 0.0027
E232D	0.204 ± 0.012	0.591 ± 0.016	16.9 ± 2.4	0.492 ± 0.045	1.80 ± 0.15	0.0757 ± 0.0051
E232Q	0.0015 ± 0.0005	0.0035 ± 0.001	nd[c]	nd[c]	nd[c]	nd[c]
E232A	nd[c]	nd[c]	nd[c]	nd[c]	nd[c]	nd[c]
D326E	32.2 ± 1.6	116 ± 2.8	18.0 ± 5.3	1.03 ± 0.12	0.932 ± 0.088	0.0387 ± 0.0031
D326N	5.72 ± 0.16	16.0 ± 0.31	14.0 ± 5.5	0.838 ± 0.062	1.48 ± 0.051	0.0210 ± 0.0015
D326A	0.0776 ± 0.0020	0.834 ± 0.014	47.4 ± 11	1.37 ± 0.082	4.27 ± 0.16	0.0458 ± 0.0048

[a] Reaction conditions: Forward, pH 9.1, saturating ATP and creatine. Reverse, pH 7.0, saturating ADP and phosphocreatine. [b] Units are in millimolar. [c] Not detected.

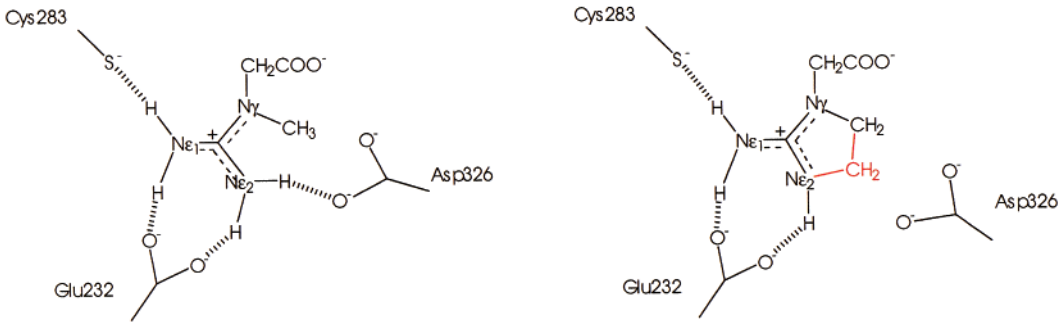

FIGURE 3: Schematic drawing of proposed interaction between HMCK and creatine or cyclocreatine. Hashed bonds represent potential hydrogen bonds. Red bonds represent the additional methylene bridge of cyclocreatine.

reaction rates. The sole exception is the D326A mutant, which has 10-fold greater activity in the reverse direction than in the forward direction.

The Michaelis constants (K_m values), shown in Table 1, show only relatively minor changes from wild-type. In the forward reaction, no significant differences in K_m were observed for E232D (Table 1). Only D326A had any noticeable increase in both K_m^{ATP} and K_m^{Cr}; about 3- and 4-fold, respectively. For the reverse reaction, D326A again possessed the most conspicuous increase in K_m^{PCr}, about 6-fold, while the E232D mutant had a 2.5-fold increase in K_m^{PCr}. From these values, it would seem that neither of these residues has a major impact on substrate interactions.

Reaction with Cyclocreatine. Of the available creatine analogues, cyclocreatine (CyCr) exhibits the most reactivity with CK (*34*). In cyclocreatine, the positions of the atoms and the bond angles fixed by the ring structure are expected to be very close to those adopted by creatine in the enzyme−substrate complex (*39*). However, the addition of a methylene bridge to form cyclocreatine fixes the stereochemistry of the two possible phosphorylation sites, which makes it possible to orient this site on the substrate relative to residues in the active-site cleft of CK (Figure 3). We studied the reaction of wild type and variant CKs with cyclocreatine with the expectation that CyCr might provide additional discrimination between the functions of the two carboxyl residues. Because phosphocyclocreatine (1-carboxymethyl-2-imino-3-phospho-4-imidazoline) is a much poorer substrate for CK than phosphocreatine (*40*), the reaction with cyclocreatine was studied only in the forward reaction. Table 2 shows that for wild-type CK the K_m for cyclocreatine is about 20 mM, i.e., about 2-fold higher than that for creatine. Substitutions with the two noncharged amino acid substitutions, D326N, and D326A, result in the phosphorylation of CyCr at equal or higher rates than those measured for the phosphorylation of Cr. In contrast, the wild-type and negatively charged CK variants, E232D and D326E, phosphorylate CyCr at only 30% of their respective Cr phosphorylation rates.

Table 2: Kinetic Parameters for Wild-Type and Recombinant HMCKs Using Cyclocreatine as Substrate

protein	k_{cat}[a] (s^{-1})	K_m^{CyCr} (mM)	k_{cat}/K_m ($s^{-1}\,M^{-1}$)	$k_{cat}^{CyCr}/k_{cat}^{Cr}$
wild-type	38.4 ± 2.7	22.8 ± 2.8	1680	0.31
E232D	0.0462 ± 0.0061	25.0 ± 2.6	1.85	0.23
D326E	10.4 ± 0.75	19.4 ± 2.7	536	0.32
D326N	6.23 ± 0.84	27.9 ± 6.4	223	1.1
D326A	0.308 ± 0.055	39.4 ± 11	7.82	2.6

[a] k_{cat} for forward reaction.

DISCUSSION

Evidence for a difference in function for the two carboxylates under investigation is provided in part by primary sequence alignments. The NEED-box region (residues 223−243 in Figure 1), in which E232 is located, is highly conserved across all members of the guanidino-kinase family for the 20 residue stretch shown in Figure 1. Conversely, the flexible loop (HMCK residues 316−338 in Figure 1), which contains D326, is only ~40% identical for all pairwise comparisons within the CK family. Moreover, this region is clearly and consistently different between the CK and AK families. The importance of this flexible loop to the overall function of all superfamily members is suggested by measurements using small-angle X-ray scattering (*37*). These show that, notwithstanding their primary structure differences, CK and AK seem to behave similarly with respect to the movement of the flexible loops upon substrate binding.

The strikingly different levels of activity loss associated with substitutions generated at these two residues also suggest different catalytic roles for each. Glu232 is intolerant of any change; even a conservative substitution (E232D), which

retains the functional group but shortens the carbon chain by a single methylene unit, results in 500-fold loss of activity. Replacement of the carboxyl group by substitution with the structurally similar but uncharged glutamine nearly eliminates activity. Consistent with these results, the nonconservative replacement of Glu232 with Ala results in complete loss of activity, within the limits of detection ($>10^{-6}$ units/mg). This trend of loss in activity is characteristic of the removal of a critical catalytic residue. Further, the log V_{max} vs pH and log V_{max}/K_m vs pH profiles for wild-type and E232D variants are very similar (data not shown). Consequently, the possibility that the activity observed for E232D is due to contamination by revertants to wild-type cannot be ruled out. In contrast, Asp326 is much more tolerant of amino acid replacement than Glu232. The conservative mutation (D326E) retains a significant proportion of the wild-type enzymatic activity. Exchange of a charged for an uncharged residue causes a significant drop (20-fold) in catalysis (D326N), while complete removal of the carboxylate group (D326A), produces an approximately 3 orders of magnitude loss of activity. Taken together these data suggest that, although Asp326 is required for optimal activity, CK can still function at a reasonable rate without it.

Assuming that the TSAC-AK structure is a suitable model for the analogous substrate-bound CK, then the flexible loop in CK should contribute to catalysis by folding from an open to a closed position, thus completing the active-site pocket and bringing into proximity residues that might contribute to catalysis (Figure 2). In the AK structure, the flexible loop residue Glu314, the putative homologue of CK Asp326, comes into proximity with the transphosphorylation site. Here it could coordinate either the guanidine or phosphoguanidine groups, thereby providing optimal alignment for in-line attack (*41*). Data from our kinetic experiments with CyCr support this concept; a decrease in k_{cat} resulting from a charged-to-nonpolar residue substitution (D326A) may be partially alleviated by a compensatory change in the substrate, i.e., the addition of the methylene bridge in CyCr (Figure 3). On the basis of these observations, we propose that in the CK mechanism, Asp326 may have a role in properly aligning the substrate by virtue of its residence on the flexible loop and the subsequent positioning of this loop proximal to the creatine or phosphocreatine molecule prior to transphosphorylation. We suggest that the differences in loop design, i.e., small nonpolar amino acids in the CK loop (HMCK residues 323−330) versus the largely negatively charged residues of the homologous AK loop (residues 312−319 in Figure 1), are likely to account for differences in substrate specificity between CK and AK.

Although the relative importance of both Glu232 and Asp326 in the HMCK mechanism have been confirmed, the details of their contributions remain unresolved. However, it is informative to view the current data in terms of earlier models of CK action. Nearly 20 years ago Cook et al. (*19*) proposed that, for RMCK, a group with a pK_a of 7 must be unprotonated in the forward reaction and protonated in the reverse reaction, thereby acting as an acid−base catalyst. On the basis of a pK_a value of 7 and an observed decrease in that pK_a during solvent perturbation experiments, this acid−base catalyst was originally proposed to be a histidine. This putative active-site histidine was proposed to facilitate catalysis by accepting a proton from or donating a proton to the Nϵ_2 of creatine and phosphocreatine, either helping to create a good nucleophile or making the phosphate on PCr a better leaving group. However, in a later study, Chen et al. (*25*) carried out a mutagenic analysis of all the conserved histidine residues in RMCK, concluding that none was essential for catalysis.

On the basis of the results described here, we now propose that Glu232 may perform the role of the acid−base catalyst that was assigned to a histidine in the earlier model (*19*). This residue was first suggested by Zhou et al. (*29*) as being a contributing feature in the AK reaction. One major concern with this hypothesis is that the pK_a of Glu232 would need to be shifted from 4 to a value of nearly 7 in order to facilitate reversible proton transfer. However, studies of other enzymes provide a precedent for the elevation of the pK_a of glutamate or aspartate residues, generally as a result of acidic or hydrophobic residues in the vicinity of the ionizable group. These include human lysozyme (*42*, *43*) and the phospholipase C reaction (*44*). On the basis of the structure of RMCK, which has 96% sequence identity with HMCK, the residues Glu231, Asp233, Pro143, Thr281, and Leu202, are potential contributors to such an elevation in pK_a for Glu232. Further, some of the substrates also carry acidic groups (ADP, ATP, or PCr) that could, upon binding, contribute to an elevated pK_a.

A complex picture of the CK reaction is now emerging from recent mutagenic and structural research. The mechanism must explain the participation of reactive glutamic acid and cysteine residues, the involvement of the flexible loop, as well as nucleotide and guanidinium binding residues, in both the forward and reverse reactions. Clearly, there must be several contributors to the overall mechanism (*45*). The AK structure provides a detailed view of a guanidino-kinase active site at the midpoint in the phosphoryl transfer reaction, which can be used to infer some mechanistic properties of other superfamily members, e.g., CKs, and guided our selection of two conserved carboxylates, Glu232 and Asp326, for amino acid replacement. Finally, between Glu232 and Asp326, our results have identified Glu232 as the acidic residue more vital for catalysis.

REFERENCES

1. Kuby, S. A., Noda, L., and Lardy, H. A. (1954) *J. Biol. Chem. 209*, 191−201.
2. Dawson, D. S., Eppenberger, H. M., and Kaplan, N. O. (1965) *Biochem. Biophys. Res. Commun. 21*, 346−353.
3. Eder, M., Fritz-Wolf, K., Kabsch, W., Wallimann, T., and Schlattner, U. (2000) *Proteins 39*, 216−225.
4. Apple, F. S. (1999) *Coronary Artery Dis. 10*, 75−79.
5. Hoosein, N. M., Martin, K. J., Abdul, M., Logothetis, C. J., and Kaddurah-Daouk, R. (1995) *Anticancer Res. 15*, 1339−1342.
6. Schiffenbauer, Y. S., Meir, G., Cohn, M., and Neeman, M. (1996) *Am. J. Physiol. 270*, C160−169.
7. Zarghami, N., Giai, M., Yu, H., Roagna, R., Ponzone, R., Katsaros, D., Sismondi, P., and Diamandis, E. P. (1996) *Br. J. Cancer 73*, 386-390.
8. Ozawa, E., Hagiwara, Y., Yoshida, M. (1999) *Mol. Cell. Biochem. 190*, 143−151.
9. David, S., Shoemaker, M., and Haley, B. E. (1998) *Brain Res. Mol. Brain Res. 54*, 276−287.
10. Aksenova, M. V., Aksenov, M. Y., Payne, R. M., Trojanowski, J. Q., Schmidt, M. L., Carney, J. M., Butterfield, D. A., and Markesbery, W. R. (1999) *Dementia Geriatr. Cognit. Disord. 10*, 158−165.

11. Zhou, H.-M., and Tsou, C.-L. (1987) *Biochim. Biophys. Acta 911*, 136−143.
12. Buechter, D. D., Medzihradszky, K. F., Burlingame, A. L., and Kenyon, G. L. (1992) *J. Biol. Chem. 267*, 2173−2178.
13. Kassab, R., Roustan, C., and Pradel, L. A. (1968*) Biochim. Biophys. Acta 167*, 308−316.
14. James, T. L., and Cohn, M. (1974) *J. Biol. Chem. 249*, 2599−2604.
15. Wood, T. D., Guan, Z., Borders, C. L., Jr., Chen, L. H., Kenyon, G. L., and McLafferty, F. W. (1998) *Proc. Natl. Acad. Sci. U.S.A. 95*, 3362−3365.
16. Pradel, L. A., and Kassab, R. (1968) *Biochim. Biophys. Acta 167*, 317−325.
17. Clarke, D. E., and Price, N. C. (1979) *Biochem. J. 181*, 467−475.
18. Rosevear, P. R., Desmeules, P., Kenyon, G. L., and Mildvan, A. S. (1981) *Biochemistry 20*, 6155−6164.
19. Cook, P. F., Kenyon, G. L., and Cleland, W. W. (1981) *Biochemistry 20*, 1204−1210.
20. Furter, R., Furter-Graves, E. M., and Wallimann, T. (1993) *Biochemistry 32*, 7022−7029.
21. Lin, L., Perryman, M. B., Friedman, D., Roberts, R., and Ma, T. S. (1994) *Biochim. Biophys. Acta 1206*, 97−104.
22. Zhou, H.-M., and Tsou, C.-L. (1985) *Biochim. Biophys. Acta 830*, 59−63.
23. Gross, M., Furter-Graves, E. M., Wallimann, T., Eppenberger, H. M., and Furter, R. (1994) *Protein Sci. 7*, 1058−1068.
24. Hagemann, H., Marcillat, O., Buchet, R., and Vial, C. (2000) *Biochemistry 39*, 9251−9256.
25. Chen, L. H., Borders, C. L., Vasquez, J. R., and Kenyon, G. L. (1996) *Biochemistry 35*, 7895−7902.
26. Fritz-Wolf, K., Schnyder, T., Wallimann, T., and Kabsch, W. (1996) *Nature 381*, 341−345.
27. Rao, J. K., Bujacz, G., and Wlodawer, A. (1998) *FEBS Lett. 439*, 133−137.
28. Eder, M., Schlattner, U., Becker, A., Wallimann, T., Kabsch, W., and Fritz-Wolf, K. (1999) *Protein Sci. 8*, 2258−2269.
29. Zhou, G., Somasundaram, T., Blanc, E., Parthasarathy, G., Ellington, W. R., and Chapman, M. S. (1998) *Proc. Natl. Acad. Sci. U.S.A. 95*, 8449−8454.
30. Chen, L. H., White, C. B., Babbitt, P. C., McLeish, M. J., and Kenyon, G. L. (2000) *J. Protein Chem. 19*, 59−66.
31. Bradford, M. M. (1976) *Anal. Chem. 72*, 248−254.
32. Tanzer, M., and Gilvarg, C. (1959) *J. Biol. Chem. 234*, 3201−3204.
33. Rosalki, S. B. (1967) *J. Lab. Clin. Med. 69*, 696−705.
34. Rowley, G. L., Greenleaf, A. L., and Kenyon, G. L. (1971) *J. Am. Chem. Soc. 93*, 5542−5551.
35. Huang, C. C., Jewett, A. I., Novak, W. R., Ferrin, T. E., Babbitt, P. C., and Klein, T. E. (2000) in *Pacific Symp. Biocomput. 2000* (Altman, R. B., Dunker, A. K., Hunter, L., and Klein, T. E., Eds.) pp 230−241, World Scientific, Singapore.
36. Ferrin, T. E., Huang, C., C., Jarvis, L. E. and Langridge, R. (1988) *J. Mol. Graphics 6*, 13−27, 36−37.
37. Forstner, M., Kriechbaum, M., Laggner, P., and Wallimann, T. (1998) *Biophys. J. 75*, 1016−1023.
38. Jacobs, H. K., and Kuby, S. A. (1980) *J. Biol. Chem. 255*, 8477−8482.
39. Phillips, G. N., Thomas Jr., J. W., Annesley, T. M., and Quiocho, F. A. (1979) *J. Am. Chem. Soc. 101*, 7120−7121.
40. Annesley, T. M., and Walker, J. B. (1977) *Biochem. Biophys. Res. Commun. 74*, 185−190.
41. Hansen, D. E., and Knowles, J. R. (1981) *J. Biol. Chem. 256*, 5967−5969.
42. Inoue, M., Yamada, H., Yasukochi, T., Kuroki, R., Miki, T., Horiuchi, T., and Imoto, T. (1992) *Biochemistry 31*, 5545−5553.
43. Muraki, M., Goda, S., Nagahora, H., and Harata, K. (1997) *Protein Sci. 6*, 473−476.
44. Martin, S. F., and Hergenrother, P. J. (1998) *Biochemistry 37*, 5755−5760.
45. Stroud, R. M. (1996) *Nat. Struct. Biol. 3*, 567−569.
46. Thompson, J. D., Higgins, D. G., and Gibson, T. J. (1994) *Nucleic Acids Res. 22*, 4673−4680.

BI0020980